Theoretical Study on σ-Bond Activation of $(HO)_2B-XH_3$ by $M(PH_3)_2$ (X = C, Si, Ge, or Sn; M = Pd or Pt). Noteworthy Contribution of the Boryl p_π Orbital to M−Boryl Bonding and Activation of the B−X σ-Bond

Shigeyoshi Sakaki,* Satoru Kai, and Manabu Sugimoto

Department of Applied Chemistry and Biochemistry, Faculty of Engineering, Kumamoto University, Kurokami, Kumamoto 860-8555, Japan

Oxidative addition of $(HO)_2B-XH_3$ to $M(PH_3)_2$ (X = C, Si, Ge, or Sn; M = Pd or Pt) was theoretically investigated with MP2-MP4(SDQ) and CCSD(T) methods. $(HO)_2B-XH_3$ easily undergoes oxidative addition to $Pt(PH_3)_2$ with a moderate activation energy for X = C and either a very small barrier or no barrier for X = Ge, Si, and Sn. Also, $(HO)_2B-SiH_3$, $(HO)_2B-GeH_3$, and $(HO)_2B-SnH_3$ undergo oxidative addition to $Pd(PH_3)_2$ with either a very small barrier or no barrier. Only the oxidative addition of $(HO)_2B-CH_3$ to $Pd(PH_3)_2$ cannot take place, but the reductive elimination of $(HO)_2B-CH_3$ from $Pd(CH_3)[B(OH)_2](PH_3)_2$ occurs with no barrier. The transition states (TS) of these oxidative additions are nonplanar except for the nearly planar TS of the oxidative addition of $(HO)_2B-CH_3$ to $Pt(PH_3)_2$. This TS structure is very sensitive to steric and electronic factors; for instance, the TS becomes nonplanar by substituting $PH_2(C_2H_5)$ for PH_3, to decrease the steric repulsion between $(HO)_2B-CH_3$ and $PH_2(C_2H_5)$. A noteworthy feature of these reactions is that the TS is much stabilized by the charge-transfer interaction between M d and $B(OH)_2$ p_π orbitals, which is the main reason for the high reactivity of $(HO)_2B-XH_3$ in the oxidative addition reaction. $Pt-B(OH)_2$ and $Pd-B(OH)_2$ bonds are much stronger than $Pt-XH_3$ and $Pd-XH_3$ bonds, respectively. This is because the $M-B(OH)_2$ bond is stabilized by the π-back-donating interaction between the empty p_π orbital of $B(OH)_2$ and the doubly occupied d_π orbital of Pt and Pd. Also, it should be noted that the trans influence of the boryl group is stronger than the very strong trans influence of silyl group.

Introduction

Organic compounds including a boryl group are expected to serve as an important intermediate in organic synthesis.[1] Pt- and Pd-catalyzed diboration of alkyne and alkene,[2] Pd-catalyzed thioboration of alkyne,[3] Pt- and Pd-catalyzed silylboration of diene and alkene,[4,5] and Pd-catalyzed stanaboration of diene[6] are very interesting and useful because two functional groups including a boryl group are incorporated into organic compounds at one time. Oxidative additions of B−B and B−X σ-bonds (X = Si or Sn) to low-valent transition metal complexes are proposed as a key elementary step to form an active species in these reactions, except for the Pd-catalyzed thioboration, in which metathesis of

RS−B(OH)₂ with a Pd(0) alkyne complex is theoretically proposed as a σ-bond activation process (see below). The oxidative addition of the B−Ge σ-bond is expected to be useful for organic synthesis of organogermane compounds, since the B−Ge oxidative addition produces an active species that might perform borylgermylation of alkyne and alkene to produce a new organogermane compound. The oxidative addition of R−B(OR)₂ is also expected to produce an active species that might carry out catalytic conversion of an organoborane to a different boryl compounds. Actually, the B−C oxidative addition to Pd(0) was postulated in Pd-catalyzed addition of aromatic compounds to α,β-unsaturated ketones and aldehydes.[7] The similar σ-bond activation of Ph−B(OH)₂ was postulated to be involved in Pd-catalyzed phenyl incorporation into an aryl group[8] and Rh-catalyzed phenyl incorporation into 1,4-conjugated enoles,[9] where not oxidative addition of the Ph−B bond but transmetalation was proposed to occur.[8]

In this regard, oxidative additions of B−B and B−X σ-bonds to transition metal complexes are important

(1) For example: (a) Burgess, K.; Ohlmeyer, M. J. *Chem. Rev.* **1991**, *91*, 1179. (b) Miyaura, N.; Suzuki, A. *Chem. Rev.* **1995**, *95*, 2457.
(2) (a) Ishiyama, T.; Matsuda, N.; Miyaura, N.; Suzuki, A. *J. Am. Chem. Soc.* **1993**, *115*, 11018. (b) Ishiyama, T.; Matsuda, N.; Murata, M.; Ozawa, F.; Suzuki, A.; Miyaura, N. *Organometallics* **1996**, *15*, 713.
(3) Ishiyama, T.; Nishijima, K. Miyaura, N.; Suzuki, A. *J. Am. Chem. Soc.* **1993**, *115*, 7219.
(4) (a) Suginome, M.; Nakamura, H.; Ito. Y. *J. Chem. Soc., Chem. Commun.* **1996**, 2777. (b) Suginome, M.; Nakamura, H.; Ito, Y. *Angew. Chem., Int. Ed. Engl.* **1997**, *36*, 2516. (c) Suginome, M.; Nakamura, H.; Matsuda, T. Ito. Y. *J. Am. Chem. Soc.* **1998**, *120*, 1229.
(5) Onozawa, S.; Hatanaka, Y.; Tanaka, M. *J. Chem. Soc., Chem. Commun.* **1997**, 1229.
(6) Onozawa, S.; Hatanaka, Y.; Choi, N.; Tanaka, M. *Organometallics* **1997**, *16*, 5389.

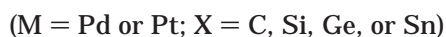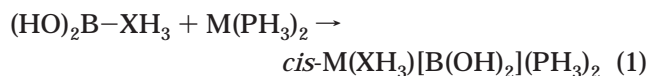(7) Cho, C. S.; Motofusa, S.; Ohe, K.; Uemura, S.; Shin, S. C. *J. Org. Chem.* **1995**, *60*, 883.
(8) Takaya, T.; Ogasawara, M.; Hayashi, T.; Sakai, M.; Miyaura, N. *J. Am. Chem. Soc.* **1998**, *120*, 5579.
(9) Aliprantis, A. O.; Canay, J. W. *J. Am. Chem. Soc.* **1994**, *116*, 6985.

subjects of research. Actually, products of B–B[10-12] and B–Sn[5a] oxidative additions have been experimentally investigated, and their X-ray structures were reported. However, no product of the other B–X oxidative addition has been experimentally investigated yet, to our knowledge, and details of these oxidative addition reactions such as geometry changes, electron distribution changes, activation energy, and reaction energy are still ambiguous.

Morokuma and his collaborators theoretically investigated Pt- and Pd-catalyzed diboration of alkenes and alkynes[13] and Pd-catalyzed thioboration of alkynes.[14] They found that B–B oxidative addition is a key elementary step in the diboration and that the thioboration of alkyne takes place not through the oxidative addition of RS–B(OR)$_2$ to Pd(0) but through the σ-bond metathesis of RS–B(OH)$_2$ with a Pd(0) alkyne complex.[14] To clarify the reaction mechanism, it is important to know whether a substrate undergoes oxidative addition to a low-valent transition metal complex. This kind of knowledge is useful in understanding the above-mentioned reactions and finding a new reaction that involves oxidative addition and reductive elimination.

In this theoretical work, we systematically investigate the oxidative additions of boryl–methyl, boryl–silyl, boryl–germyl, and boryl–stannyl bonds to platinum-(0) and palladium(0) complexes (eq 1),

$$(HO)_2B–XH_3 + M(PH_3)_2 \rightarrow$$
$$\textit{cis-}M(XH_3)[B(OH)_2](PH_3)_2 \quad (1)$$

$$(M = Pd \text{ or } Pt; X = C, Si, Ge, \text{ or } Sn)$$

where we adopt B(OH)$_2$ as a model of a pinacol–boryl group because the pinacol group is used as a substituent on the B atom in many experimental works.[1-4] Also, we adopted M(PH$_3$)$_2$ (M = Pd or Pt) as a model of platinum and palladium complexes, because platinum and palladium phosphine complexes have been used as catalysts for silylboration and stanaboration of alkynes and dienes.[4-6] Our purposes here are to clearly show how easily borylmethane, borylsilane, borylgermane, and borylstannane undergo oxidative addition to M-(PH$_3$)$_2$, to present detailed knowledge of the reaction such as geometry changes, electron distribution changes, activation energy, and reaction energy, and to make a comparison of reactivity among B–C, B–Si, B–Ge, and B–Sn σ-bonds.

Computational Details

Geometries of reactants, transition states, and products were optimized with the MP2 method, where the geometry of PH$_3$ was taken from the experimental structure of the free PH$_3$ molecule.[15] MP4SDQ and CCSD(T) calculations were carried out with those optimized geometries to estimate energy

changes in the reaction. In the CCSD(T) calculations, the contribution of triple excitations was estimated through the perturbation method using the CCSD wave function.[16]

Two kinds of basis set systems were employed here. In the smaller basis set system (BS-I), core electrons of Pt (up to 4f),[17] P (up to 2p), Si (up to 2p), Ge (up to 3d), and Sn (up to 4d)[18a] were replaced with effective core potentials (ECPs). Valence electrons of Pt and Pd were represented with (311/311/21) and (311/311/31) sets,[17] respectively, and those of P, Si, Ge, and Sn were represented with a (21/21/1)[18] set. For B, C, O, and H atoms, MIDI-3[19] and (31)[20] sets were employed, respectively, where a d polarization function[21] was added to B and C. This BS-I system was used for geometry optimization. In the larger basis set system (BS-II), valence electrons of Pt and Pd were represented with slightly more flexible (541/541/111) and (541/541/211) sets,[22] respectively, where the same ECPs as those adopted in BS-I were used. For P and Sn, the same ECPs and the same basis sets as those of BS-I were employed here. Huzinage–Dunning (721/41) sets were employed for C, O, and B, where a d polarization function was added on C and B.[20] For Si and Ge, (631111/42111/1) and (63111111/3331111/41) sets were used, respectively.[23] This BS-II system was used for estimation of energy change. The Gaussian 94 program[24] was employed for these calculations.

Results and Discussion

Geometry Changes in the Oxidative Addition of (HO)$_2$B–XH$_3$ to Pt(PH$_3$)$_2$ and Pd(PH$_3$)$_2$. Geometry changes in the oxidative additions of (HO)$_2$B–CH$_3$ and (HO)$_2$B–GeH$_3$ to Pt(PH$_3$)$_2$ are shown in Figure 1. In the precursor complex **PC1a** of the oxidative addition of (HO)$_2$B–CH$_3$, the Pt–B distance is shorter than the Pt–C distance. This is because the boryl group has an empty p$_\pi$ orbital which interacts with the doubly occupied d$_\sigma$ orbital of Pt, as will be discussed below in more detail. In the transition state **TS1a**, the dihedral angle between the B–C bond and the Pt(PH$_3$)$_2$ plane is 20°; in other words, **TS1a** is nearly planar, unlike the transition state of the C–C oxidative addition to Pt-(PH$_3$)$_2$, in which the dihedral angle was calculated to be about 80°.[25] In the product **PRO1a**, the Pt–B distance (2.034 Å) agrees well with the experimental value of similar Pt(II) diboryl complexes.[10,11] The Pt–CH$_3$ distance (2.113 Å) also agrees well with the experimentally reported Pt–alkyl distance.[26]

(10) Iverson, C. N.; Smith, M. R. *J. Am. Chem. Soc.* **1995**, *117*, 4403.
(11) Leskey, G.; Nguyen, P.; Taylor, N. J.; Marder, T. B.; Scott, A. J.; Clegg, W.; Norman, N. C. *Organometallics* **1996**, *15*, 5137.
(12) Dai, C.; Stringer, G.; Marder, T. B.; Scott, A. J.; Clegg, W.; Norman, N. C. *Inorg. Chem.* **1997**, *36*, 272.
(13) (a) Cui, Q.; Musaev, D. G.; Morokuma, K. *Organometallics* **1997**, *16*, 1355. (b) Cui, Q.; Musaev, D. G.; Morokuma, K. *Organometallics* **1998**, *17*, 742.
(14) Cui, Q.; Musaev, D. G.; Morokuma, K. *Organometallics* **1998**, *17*, 1383.
(15) Herzberg, G. *Molecular Spectra and Molecular Structure*; D. Von Nostrand Co. Inc.: Princeton, NJ, 1967; Vol. 3, p 610.
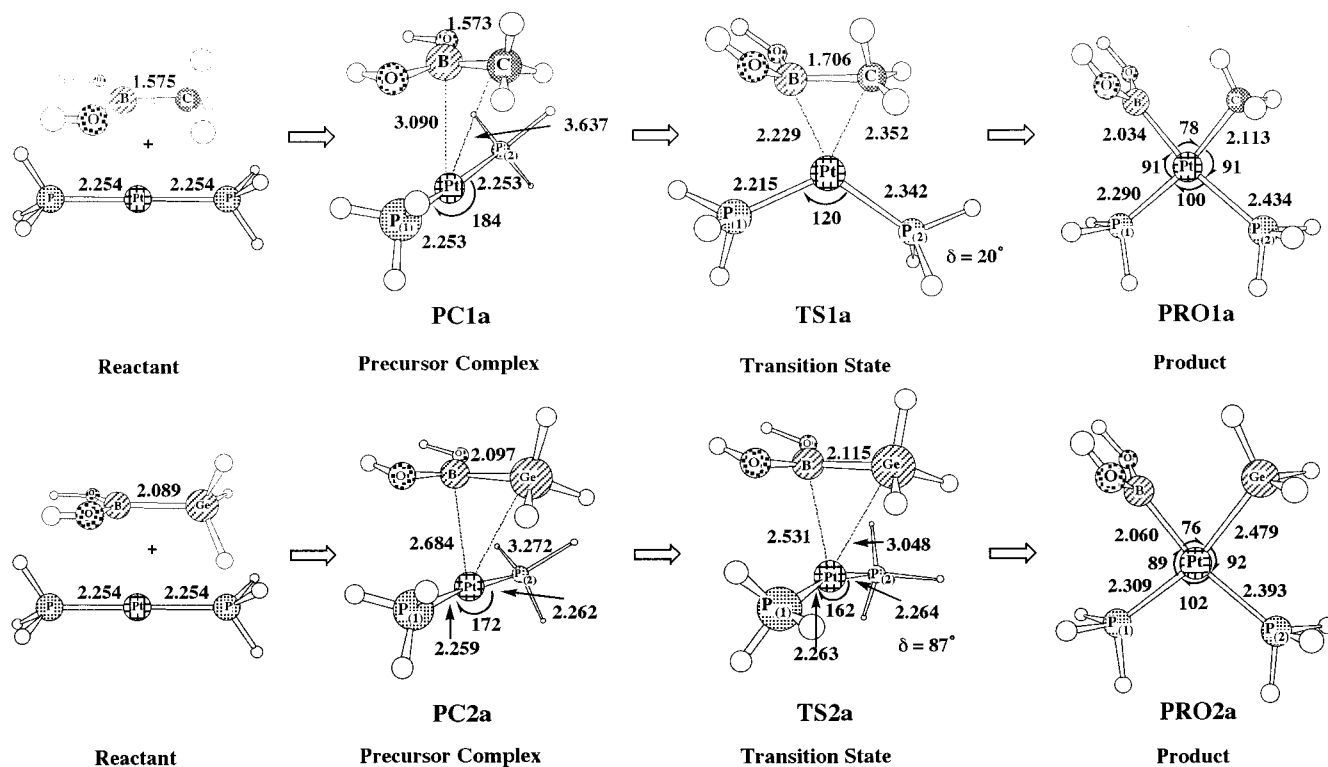
(16) Pople, J. A.; Head-Gordon, M.; Raghavachari, K. *J. Chem. Phys.* **1987**, *87*, 5968.
(17) Hay, P. J.; Wadt, W. R. *J. Chem. Phys.* **1985**, *82*, 299.
(18) (a) Wadt, W. R.; Hay, P. J. *J. Chem. Phys.* **1985**, *82*, 284. (b) Hollwarth, A.; Bohme, M.; Dapprich, S.; Ehlers, A. W.; Gobbi, A.; Jonas, V.; Kohler, K. F.; Stegmann, R.; Veldkamp, A.; Frenking, G. *Chem. Phys. Lett.* **1993**, *208*, 237.
(19) Huzinaga, S.; Andzelm, J.; Klobukowski, M.; Radzio-Andzelm, E.; Sakai, Y.; Tatewaki, H. *Gaussian Basis Sets for Molecular Calculations*; Elsevier: Amsterdam, 1984.
(20) Dunning, T. H.; Hay, P. J. In *Methods of Electronic Structure Theory*; Schaeffer, H. F., Ed.; Plenum: New York, 1977; p 1.
(21) Sakai, Y.; Tatewaki, H.; Huzinaga, S. *J. Comput. Chem.* **1981**, *2*, 108.
(22) Couty, M.; Hall, M. B. *J. Comput. Chem.* **1996**, *17*, 1359.
(23) McLean, A. D.; Chandler, G. S. *J. Chem. Phys.* **1980**, *72*, 5639.
(24) Frisch, A. M. J.; Trucks, G. W.; Schlegel, H. B.; Gill, P. M. W.; Johnson, B. G.; Robb, M. A.; Cheeseman, J. R.; Keith, T. A.; Petersson, G. A.; Montgomery, J. A.; Raghavachari, K.; Al-Laham, M. A.; Zakrzewski, V. G.; Ortiz, J. V.; Foresman, J. B.; Cioslowski, J.; Stefanov, B. B.; Nanayakkara, A.; Challacombe, M.; Peng, C. Y.; Ayala, P. Y.; Chen, W.; Wong, M. W.; Andres, J. L.; Replogle, E. S.; Gomperts, R.; Martin, R. L.; Fox, D. J.; Binkley, J. S.; DeFrees, D. J.; Baker, J.; Stewart, J. J. P.; Head-Gordon, M.; Gonzalez, C.; Pople, J. A. *Gaussian 94*; Gaussian Inc.: Pittsburgh, PA, 1995.
(25) Sakaki, S.; Mizoe, N.; Musashi, Y.; Biswas, B.; Sugimoto, M. *J. Phys. Chem. A* **1998**, *102*, 8027.

Figure 1. Geometry changes of oxidative additions of (HO)$_2$B−CH$_3$ and (HO)$_2$B−GeH$_3$ to Pt(PH$_3$)$_2$. Bond distances in angstroms and bond angles in degrees.

In the precursor complex **PC2a** of the oxidative addition of (HO)$_2$B−GeH$_3$, the Pt−B distance is shorter than the Pt−Ge distance, too. The Pt−B and Pt−Ge distances are shorter than the Pt−B and Pt−C distances in **PC1a**, respectively, suggesting that (HO)$_2$B−GeH$_3$ is more electron-accepting than (HO)$_2$B−CH$_3$. The transition state **TS2a** is nonplanar, and the dihedral angle between the B−Ge bond and the Pt(PH$_3$)$_2$ plane is about 90°, like the transition state of the Si−C oxidative addition to Pt(PH$_3$)$_2$.[25] The Ge−B distance slightly lengthens to 2.115 Å at **TS2a**, which is only 0.026 Å longer than that of the free (HO)$_2$B−GeH$_3$ molecule. The Pt−B and Pt−Ge distances are still much longer than those of the product **PRO2a**. These features indicate that **TS2a** is reactant-like.

In oxidative additions of (HO)$_2$B−SiH$_3$ and (HO)$_2$B−SnH$_3$, we failed to optimize the transition state. The geometry changes in these oxidative additions were optimized as a function of the Pt−B distance, as shown in Figure 2, where we arbitrarily adopt the Pt−B distance as a reaction coordinate since B(OH)$_2$ more closely approaches Pt than CH$_3$ and GeH$_3$ in the precursor complexes **PC1a** and **PC2a** and the transition states **TS1a** and **TS2a**. Apparently, the total energy monotonically decreases as the Pt−B distance becomes shorter and, in particular, steeply decreases when the Pt−B distance becomes shorter than about 2.5 Å. The similar energy change was observed in the oxidative addition of (HO)$_2$B−SnH$_3$, while its results are omitted for brevity; geometries of products **PRO3a** and **PRO4a** are shown in Figure 3. From these results, it is reason-
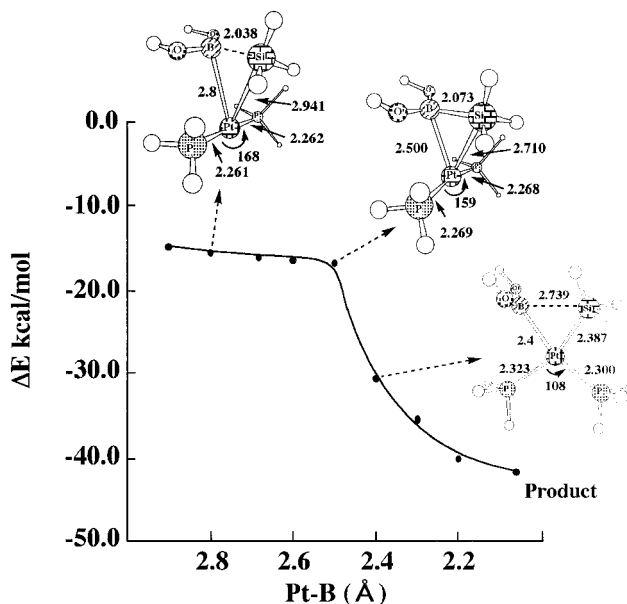
(26) For instance, R(Pt−CH$_3$) = 2.113 Å in *cis*-Pt(CH$_3$)(SiPh$_3$)-(PMePh$_2$)$_2$, which is considered a reasonable model of *cis*-Pt(CH$_3$)-[B(OH)$_2$](PH$_3$)$_2$ since the trans influence of B(OH)$_2$ is very strong (see text). Ozawa, F.; Hikida, T.; Hayashi, T. *J. Am. Chem. Soc.* **1994**, *116*, 2844.

Figure 2. Geometry and energy changes of oxidative addition of (HO)$_2$B−SiH$_3$ to Pt(PH$_3$)$_2$. Bond distances in angstroms and bond angles in degrees. Energy zero is taken for the infinite separation between Pt(PH$_3$)$_2$ and (HO)$_2$B−CH$_3$.

ably concluded that the oxidative additions of (HO)$_2$B−SiH$_3$ and (HO)$_2$B−SnH$_3$ to Pt(PH$_3$)$_2$ occur with no barrier.

Interesting features are observed in these products: (1) the Pt−P(2) bond at a position trans to B(OH)$_2$ is considerably longer than the other Pt−P(1) bond at a position trans to CH$_3$, SiH$_3$, and GeH$_3$ (see Figures 1 and 3), and (2) the Pt−P(1) bond positioned trans to XH$_3$ becomes shorter in the order SiH$_3$ ≈ SnH$_3$ > GeH$_3$ >
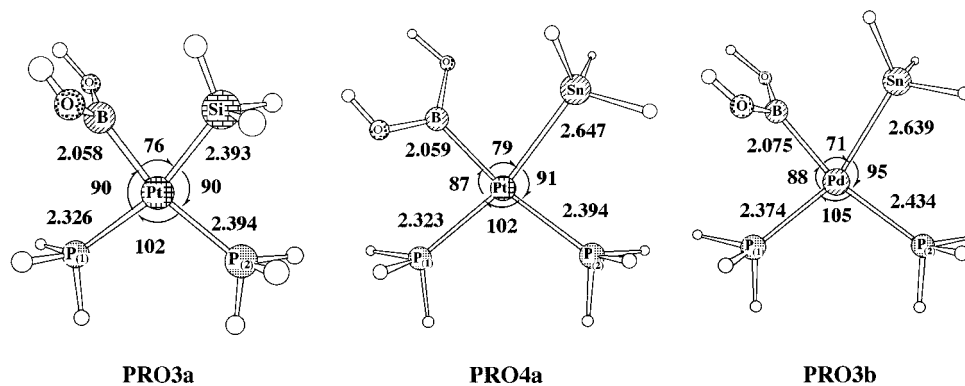
Figure 3. Geometries of Pt(SiH₃)[B(OH)₂](PH₃)₂, Pt(SnH₃)[B(OH)₂](PH₃)₂, and Pd(SnH₃)[B(OH)₂](PH₃)₂. Bond distances in angstroms and bond angles in degrees.
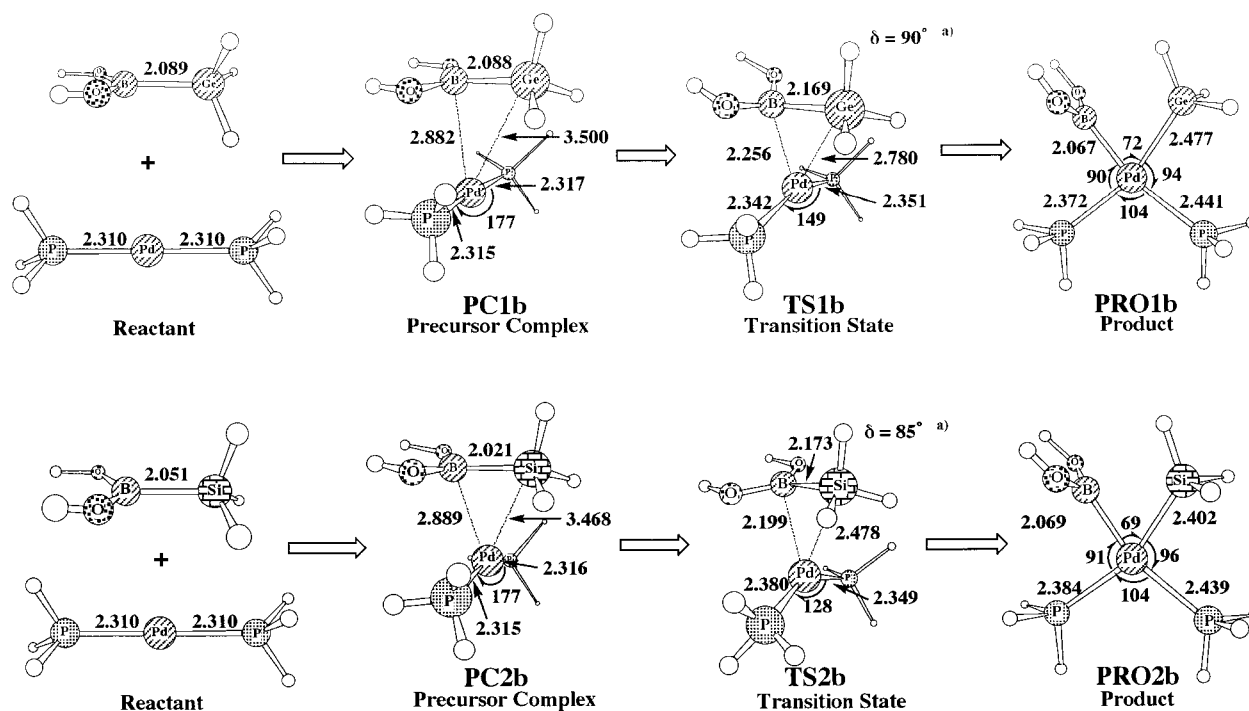

Figure 4. Geometry changes of oxidative additions of $(HO)_2B-SiH_3$ and $(OH)_2B-GeH_3$ to $Pd(PH_3)_2$. Bond distances in angstroms and bond angles in degrees.

CH₃. These results indicate that the trans influence becomes weaker in the order $B(OH)_2 > SiH_3 \approx SnH_3 > GeH_3 > CH_3$, and the $B(OH)_2$ ligand exhibits very strong trans influence. The $B-Pt-X$ angle is somewhat smaller than 90°. A similar feature was reported in the X-ray structures of $Pt[B(OR)_2]_2(PR_3)_2$[10−12] and $Pd(SnR_3)[B(OR)_2]$-$(PR_3)_2$.[5a]

Geometry changes in oxidative additions of $(HO)_2B-SiH_3$ and $(HO)_2B-GeH_3$ to $Pd(PH_3)_2$ are shown in Figure 4. In the precursor complex **PC1b**, $(HO)_2B-GeH_3$ is more distant from Pd than that in **PC2a**, probably because $Pt(PH_3)_2$ can form a stronger charge-transfer interaction with $(HO)_2B-GeH_3$ than does Pd-$(PH_3)_2$. In both transition states **TS1b** and **TS2b**, the Si−B and Ge−B bonds are almost perpendicular to the $Pd(PH_3)_2$ plane. These transition states are considered reactant-like, since the B−Si and B−Ge bonds to be broken in the reaction lengthen a little. In the oxidative addition of $(HO)_2B-SnH_3$, we failed to optimize the transition state but could optimize easily the product (see Figure 3). The geometry changes in this oxidative addition were calculated as a function of the Pd−B

distance, in which the total energy monotonically decreases as the B−Sn distance becomes shorter, like that of Figure 2 (the results are omitted to save space). These results indicate that this reaction occurs with no barrier. The Pd−Si, Pd−Ge, and Pd−B distances of **PRO2b** and **PRO1b** are almost the same as the Pt−Si, Pt−Ge, and Pt−B distances in **PRO3a**, **PRO2a**, and **PRO1a**, respectively, while the Pd−P distance is considerably longer than the Pt−P distance. In **PRO1b** and **PRO2b**, the Pd−P(2) bond at a position trans to $B(OH)_2$ is longer than the Pd−P(1) bond at a position trans to GeH_3 or SiH_3. Also, the Pd−P(1) bond positioned trans to SiH_3, GeH_3, and SnH_3 becomes shorter in the order $SiH_3 > SnH_3 > GeH_3$. From these results, it is also concluded in Pd(II) complexes that the trans influence becomes weaker in this order and the trans influence of boryl is very strong.

In the oxidative addition of $(HO)_2B-CH_3$, we failed to optimize the geometry of $Pd(CH_3)[B(OH)_2](PH_3)_2$; this complex converts to the precursor $Pd[(HO)_2B-CH_3]$-$(PH_3)_2$ in the optimization. $Pd(CH_3)[B(OH)_2](PH_3)_2$ is much less stable than the precursor complex by 25.7

187.5*i*cm⁻¹   **73.9*i*cm⁻¹**   **67*i*cm⁻¹**

(A) Oxidative Addition of   **(B) Oxidative Addition of**   **(C) Oxidative Addition of**
(HO)₂B·CH₃ to Pt(PH₃)₂   **(HO)₂B-GeH₃ to Pt(PH₃)₂**   **(HO)₂B-GeH₃ to Pd(PH₃)₂**
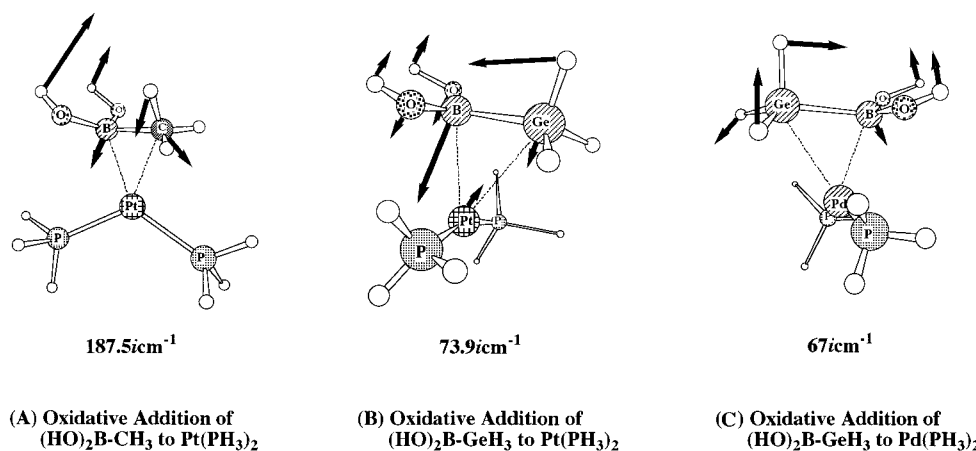
Figure 5. Vibrational frequencies of the transition states and important geometry changes involved in the eigenvector with imaginary frequency. The numbers are imaginary frequencies (MP2/BS-I).

kcal/mol (MP4SDQ/BS II), where Pd(CH₃)[B(OH)₂]-(PH₃)₂ was optimized under the assumption that the BPdC angle was fixed to be the same as that of **PRO1a**. These results indicate that (HO)₂B−CH₃ cannot undergo oxidative addition to Pd(PH₃)₂, but the reductive elimination of (HO)₂B−CH₃ from the Pd(II) complex occurs with no barrier.

Some of these transition states were ascertained with vibrational frequency calculation, and eigenvectors with imaginary frequency are schematically shown in Figure 5.[27] It should be noted that the absolute value of the imaginary frequency is not large (67i to 74i cm⁻¹) in the oxidative addition of the Ge−B bond. In the eigenvector with imaginary frequency, B−Ge bond breaking is not involved, but direction changes of B(OH)₂ and GeH₃ groups are observed. These features clearly indicate that bond breaking does not occur at the TS, which is consistent with the reactant-like structure of the transition state. In the oxidative addition of (HO)₂B−CH₃ to Pt(PH₃)₂, on the other hand, the absolute value of the imaginary frequency is rather large (188i cm⁻¹). In the eigenvector with this frequency, not only the direction changes of the B(OH)₂ and CH₃ groups but also the stretching of the B−C bond are observed, indicating that the B−C bond begins to break in this TS. This means that the B−C bond-breaking process contributes to the activation barrier.

Activation Energy (E_a) and Reaction Energy (ΔE). The activation energy (E_a) is defined as the energy difference between the precursor complex and the transition state, and the reaction energy (ΔE) is the energy difference between the product and the sum of reactants. The negative value of ΔE means that the reaction is exothermic. As shown in Table 1, E_a and ΔE were calculated with various computational methods. Although E_a and ΔE moderately fluctuate at MP2, MP3, and MP4DQ, they change little upon going to CCSD(T) from MP4SDQ, indicating that the MP4SDQ method is useful here. Thus, we present our discussion based on the MP4SDQ values.

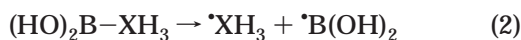As apparently shown in Table 2, (HO)₂B−GeH₃ undergoes oxidative addition to both Pt(PH₃)₂ and Pd-

(27) Besides these frequencies shown in Figure 5, several imaginary frequencies were calculated. However, all of them are corresponding to PH₃ rotations. Moreover, they are separated well from the imaginary frequency shown in Figure 5. Thus, the frequencies of Figure 5 seem reasonable for the transition state.

Table 1. Correlation Effects on an Activation Energy (E_a)[a] and a Reaction Energy (ΔE)[b] (kcal/mol) of Oxidative Addition of (HO)₂B−GeH₃ to Pt(PH₃)₂

	E_a	ΔE
MP2	1.3	−38.0
MP3	2.8	−30.4
MP4DQ	2.4	−32.2
MP4SDQ	1.9	−33.1
CCSD(T)	1.9	−33.4

[a] E_a = energy difference between the TS and the precursor complex. [b] ΔE = energy difference between the product and the sum of reactants.

Table 2. Activation Energy (E_a)[a] and Reaction Energy (ΔE)[b] of Oxidative Addition of (HO)₂B−XH₃ to M(PH₃)₂ (M = Pd or Pt) (MP4SDQ/BS-II Method, kcal/mol unit)

(A) Oxidative Additions to Pd(PH₃)₂				
XH₃	CH₃	SiH₃	GeH₃	SnH₃
E_a		1.2	1.1	no[c]
ΔE	25.7	−13.7	−14.1	−22.4

(B) Oxidative Additions to Pt(PH₃)₂						
XH₃	CH₃	SiH₃	GeH₃	SnH₃	CH₃−CH₃[d]	SiH₃−CH₃[d]
E_a	21.5	no[c]	2.2	no[c]	57.4	19.5
ΔE	3.0	−33.0	−33.9	−39.4	7.6	−7.1

[a] E_a = energy difference between the TS and the precursor complex. [b] ΔE = energy difference between the product and the sum of reactants. [c] The reaction occurs with no barrier. [d] Ref 25.

(PH₃)₂ with a very small activation energy. (HO)₂B−SnH₃ undergoes oxidative addition to both Pt(PH₃)₂ and Pd(PH₃)₂ with no barrier. The oxidative addition of (HO)₂B−SiH₃ to Pt(PH₃)₂ occurs with no barrier and that to Pd(PH₃)₂ with a small activation energy. All these oxidative additions to Pt(PH₃)₂ are significantly exothermic, while the oxidative additions to Pd(PH₃)₂ are much less exothermic. On the other hand, the oxidative addition of (HO)₂B−CH₃ to Pt(PH₃)₂ needs a moderate activation energy of 22 kcal/mol, while its endothermicity is very small (3 kcal/mol). This oxidative addition to Pd(PH₃)₂ cannot occur, but the reductive elimination takes place with no barrier. From these results, it should be reasonably concluded that (HO)₂B−SiH₃, (HO)₂B−GeH₃, and (HO)₂B−SnH₃ are significantly reactive for the oxidative addition, but (HO)₂B−CH₃ is much less reactive than the others. Also,

$Pd(PH_3)_2$ is less reactive for oxidative addition than $Pt(PH_3)_2$. Usually, the oxidative addition to a Pd(0) complex does not easily occur due to the stable d orbital energy.[28,29] This is the reason for the lower reactivity of the Pd(0) complex for the oxidative addition, as mentioned above.

Nevertheless, oxidative additions of $(HO)_2B-SiH_3$, $(HO)_2B-GeH_3$, and $(HO)_2B-SnH_3$ to $Pd(PH_3)_2$ occur with either a very small activation barrier or no barrier like those to $Pt(PH_3)_2$. This is surprising. The exothermicity of these oxidative additions is much less than those of the oxidative additions to $Pt(PH_3)_2$, as mentioned above. Thus, the product stability is not responsible for the low activation energy observed in oxidative additions of $(HO)_2B-SiH_3$, $(HO)_2B-GeH_3$, and $(HO)_2B-SnH_3$ to $Pd(PH_3)_2$. Some stabilizing interaction at the transition state would play a role to lower the activation energy. Such stabilizing interaction will be analyzed below in detail by inspecting electron distribution and bonding nature at the TS.

Interesting differences between $(HO)_2B-CH_3$ and CH_3-CH_3 are also worthy of note, as follows: (1) although the endothermicity is similar in the oxidative additions of these two substrates to $Pt(PH_3)_2$, the oxidative addition of $(HO)_2B-CH_3$ occurs with a much lower E_a value than that of CH_3-CH_3, as shown in Table 2, and (2) the TS structure of the CH_3-CH_3 oxidative addition is nonplanar,[25] but that of $(HO)_2B-CH_3$ is nearly planar. Similar differences are observed between the oxidative additions of CH_3-SiH_3 and $(HO)_2B-SiH_3$ to $Pt(PH_3)_2$; the oxidative addition of $(HO)_2B-SiH_3$ occurs with no barrier and significant exothermicity, while that of CH_3-SiH_3 requires a considerably large activation energy[25] (see Table 2). These differences are also interpreted in terms of the above-mentioned stabilizing interaction at the transition state, which will be discussed below.

Comparison of $M-B(OH)_2$, $M-CH_3$, $M-SiH_3$, $M-GeH_3$, and $M-SnH_3$ Bond Energies. The reaction energy is directly related to the bond energies. In these oxidative addition reactions, the B-X bond is broken but the $M-B(OH)_2$ and $M-XH_3$ bonds are formed. To understand not only the reaction energy value but also the bond nature, the bond energy value is fundamental information. We estimated two kinds of bond energy: one is the first bond dissociation energy and the other is the average bond energy. The former is estimated by considering eqs 2 and 3:

$$(HO)_2B-XH_3 \rightarrow {}^{\bullet}XH_3 + {}^{\bullet}B(OH)_2 \qquad (2)$$

$$PtH(XH_3)(PH_3)_2 \rightarrow {}^{\bullet}PtH(PH_3)_2 + {}^{\bullet}XH_3 \qquad (3)$$

The latter is estimated by considering eqs 4 and 5:

$$Pt(XH_3)_2(PH_3)_2 \rightarrow Pt(PH_3)_2 + X_2H_6 \qquad (4)$$

$$PtH\{B(OH)_2\}(PH_3)_2 \rightarrow Pt(PH_3)_2 + H-B(OH)_2 \qquad (5)$$

(28) Sakaki, S.; Ogawa, M.; Kinoshita, M. *J. Phys. Chem.* **1995**, *99*, 9933.

(29) A similar discussion was presented previously by Goddard et al. They theoretically investigated the reductive elimination of CH_3-CH_3 from $M(CH_3)_2(PH_3)_2$ (M = Pd or Pt) and explained the reactivity difference between Pd and Pt in terms of the d^{10} to d^9s promotion energy. Low, J. J.; Goddard, W. A. *J. Am. Chem. Soc.* **1986**, *108*, 6115.
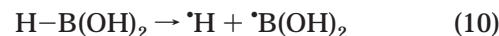
Table 3. First Bond Dissociation Energies and the Average Bond Energies (kcal/mol)

(A) First Bond Dissociation Energy

	MP2	MP3	MP4DQ	MP4SDQ
$(HO)_2B-CH_3$	111.5	110.4	109.5	109.7
$(HO)_2B-SiH_3$	87.8	87.8	86.5	86.8
$(HO)_2B-GeH_3$	83.8	83.2	83.0	83.5
$(HO)_2B-SnH_3$	73.1	72.8	72.4	72.8
$Pt-B(OH)_2$	92.6	87.1	88.5	89.1
$Pt-CH_3$	70.8	64.2	64.9	65.5
$Pt-SiH_3$	82.2	76.1	78.2	78.6
$Pt-GeH_3$	78.4	72.0	74.4	75.0
$Pt-SnH_3$	75.0	67.9	70.7	71.2
$Pd-B(OH)_2$	81.1	70.9	75.3	77.0
$Pd-CH_3$	60.8	50.4	53.2	54.3
$Pd-SiH_3$	78.2	66.8	72.4	74.6
$Pd-GeH_3$	73.6	62.3	67.9	69.8
$Pd-SnH_3$	73.6	61.9	67.8	69.7

(B) Average Bond Energy

	MP2	MP3	MP4DQ	MP4SDQ
$Pt-B(OH)_2$	63.4	63.4	63.7	64.4
$Pt-CH_3$	46.8	42.0	41.7	42.4
$Pt-SiH_3$	56.5	52.7	53.6	54.2
$Pt-GeH_3$	53.0	48.4	50.0	50.7
$Pt-SnH_3$	48.9	43.7	45.6	46.3
$Pd-B(OH)_2$	55.0	50.9	51.8	52.8
$Pd-CH_3$	33.9	29.2	28.8	29.4
$Pd-SiH_3$	46.2	41.7	43.4	44.1
$Pd-GeH_3$	44.0	39.6	41.5	42.3
$Pd-SnH_3$	41.9	37.1	39.3	40.3

Since the reaction energy ΔE_4 of eq 4 is represented by eq 6, the $E(Pt-XH_3)$ value is estimated by adding $E(X-X)$ to ΔE_4, where the $E(X-X)$ value used was evaluated with eq 8. The reaction energy ΔE_5 of eq 5 is represented by eq 7. We easily evaluate $E[Pt-B(OH)_2]$ by adding $E(M-H)$ and $E[H-B(OH)_2]$ to ΔE_5, where $E(M-H)$ and $E[H-B(OH)_2]$ values were evaluated with eqs 9 and 10, respectively.

$$\Delta E_4 = 2E(Pt-XH_3) - E(X-X) \qquad (6)$$

$$\Delta E_5 = E[Pt-B(OH)_2] + E(M-H) - E[H-B(OH)_2] \qquad (7)$$

$$X_2H_6 \rightarrow 2\,{}^{\bullet}XH_3 \qquad (8)$$

$$M(H)_2(PH_3)_2 \rightarrow M(PH_3)_2 + H_2 \qquad (9)$$

$$H-B(OH)_2 \rightarrow {}^{\bullet}H + {}^{\bullet}B(OH)_2 \qquad (10)$$

As shown in Table 3, these bond energies fluctuate little upon going from MP2 to MP4SDQ, as has been reported previously.[25,30] Therefore, we discuss here the bond energy calculated with the MP4SDQ method.

As expected, both the first bond dissociation energy and the average bond energy of the B-X bond decrease in the order B-C ≫ B-Si > B-Ge > B-Sn, as shown in Table 3. The $M-B(OH)_2$ bond is much stronger than the $M-XH_3$ bond and the B-C bond is much stronger than the C-C bond, unexpectedly. Despite the strong B-C bond, the B-C oxidative addition to $Pt(PH_3)_2$ proceeds with exothermicity similar to that of the C-C oxidative addition (vide supra). This is easily interpreted in terms that the $Pt-B(OH)_2$ bond is much stronger than the $M-CH_3$ bond. However, the B-C oxidative

(30) Sakaki, S.; Biswas, B.; Sugimoto, M. *Organometallics* **1998**, *17*, 1278.

Scheme 1
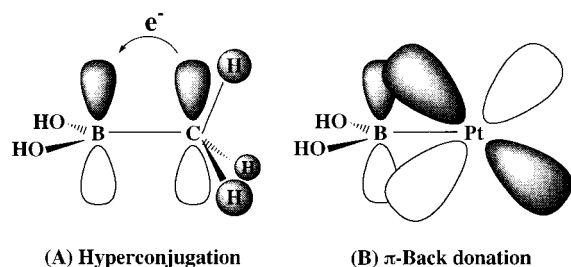
(A) Hyperconjugation   **(B) π-Back donation**

**Table 4. Natural Bond Orbital (NBO) Population[a]
of the B p_π Orbital**

•B(OH)₂	(HO)₂B−CH₃	(HO)₂B−SiH₃	(HO)₂B−GeH₃	(HO)₂B−SnH₃
0.287	0.316	0.330	0.332	0.333

Pt(SiH₃)[B(OH)₂](PH₃)₂[b]	Pd(SiH₃)[B(OH)₂](PH₃)₂[b]
0.362	0.355

[a] At the MP2 level. [b] Geometries were taken to separate σ and π spaces.

addition to Pd(PH₃)₂ cannot occur because the Pd−CH₃ and Pd−B(OH)₂ bonds are much weaker than the Pt−CH₃ and Pt−B(OH)₂ bonds, respectively. The oxidative additions of B−Si, B−Ge, and B−Sn bonds are significantly exothermic, because M−SiH₃, M−GeH₃, M−SnH₃, and M−B(OH)₂ bonds are very strong, but B−Si, B−Ge, and B−Sn bonds are very weak (see Table 3).

Why is the B−C bond much stronger than the C−C bond? We can easily find the reason by considering the p_π orbital of the boryl group. The p_π orbital of boryl is empty in a formal sense, while it has a small electron population of 0.267e in •B(OH)₂ due to the p_π−p_π interaction between B and O atoms, where natural bond orbital populations[31] are given herewith. This small p_π orbital population indicates that the boryl p_π orbital is able to accept electrons. Thus, hyperconjugation between B p_π and C−H σ orbitals is formed, as shown in Scheme 1A. Actually, the B p_π orbital population increases to 0.316e in (HO)₂B−CH₃ (Table 4). Also, this hyperconjugation is clearly observed in the contour map of the HOMO, as shown in Figure 6. Since this interaction participates in the B−C bonding in addition to the σ-bonding interaction, the B−C bond is much stronger than the C−C bond. However, this hyperconjugation is weakly observed in the B−Si bond (see Figure 6 B) and disappears in the B−Ge and B−Sn bonds (see Figure 6C,D). Despite the absence of hyperconjugation, the B p_π orbital is observed in the occupied space in (HO)₂B−GeH₃ and (HO)₂B−SnH₃, and the p_π orbital population increases in the order •B(OH)₂ < (HO)₂B−CH₃ < (HO)₂B−SiH₃ ≈ (HO)₂B−GeH₃ ≈ (HO)₂B−SnH₃ (Table 4). This means that not hyperconjugation but intramolecular charge-transfer occurs from SiH₃, GeH₃, and SnH₃ to the B p_π orbital, and this charge-transfer interaction contributes to the B−Si, B−Ge, and B−Sn bonding. The absence of hyperconjugation in (HO)₂B−GeH₃ and (HO)₂B−SnH₃ is not surprising because the π-type interaction becomes difficult in general upon going down in the periodic table.

(31) Reed, A. E.; Weinstock, R. B.; Weinhold, F. *J. Chem. Phys.* **1985**, *83*, 735. Reed, A. E.; Curtis, L. A.; Weinhold, F. *Chem. Rev.* **1988**, *88*, 899.

**Table 5. HOMO Energy Levels (ϵ_{HOMO}) (eV) and
Ionization Potentials (I_p) (eV)**

	ϵ_{HOMO}	I_p
•B(OH)₂	−9.6	6.3
•CH₃	−10.4	9.4
•SiH₃	−9.0	7.8
•GeH₃	−8.9	7.5
•SnH₃	−8.6	7.3
•PdH(PH₃)₂	−7.0	6.4
•PtH(PH₃)₂	−6.8	6.0

It is worthwhile to investigate reasons that the M−B(OH)₂ bond is much stronger than the M−CH₃ bond. The B p_π orbital population in M(XH₃)[B(OH)₂]-(PH₃)₂ is much larger than that in •B(OH)₂, as shown in Table 4. This clearly shows that the π-back-donating interaction (Scheme 1B) between M d_π and B p_π orbitals contributes to the Pt−B(OH)₂ bond. Interestingly, the B p_π orbital population of the Pt complex is larger than that of the Pd complex, indicating that the π-back-donating interaction is stronger in the Pt complex than in the Pd complex. This is because the Pt d orbital lies at a higher energy than the Pd d orbital.[28]

A comparison of the M−CH₃ bond with M−SiH₃, M−GeH₃, and M−SnH₃ bonds is also interesting. In our previous work,[30] we reported that the Pd−alkyl bond becomes stronger by introduction of an electron-withdrawing substituent on the sp³ C atom and presented a clear explanation based on eq 11, where ΔE_{bond} represents the stabilization energy by covalent bond formation, ϵ_A and ϵ_B are orbital energies of metal valence and alkyl sp³ orbitals, respectively, and β is an usual resonance integral.

$$\Delta E_{bond} = \epsilon_A - \epsilon_B + 2\beta^2/(\epsilon_A - \epsilon_B) \qquad (11)$$

When the $|\beta|$ value is smaller than the ($\epsilon_A - \epsilon_B$) value, the ΔE_{bond} value increases as the ($\epsilon_A - \epsilon_B$) term becomes large. Since the metal d orbital is at a much higher energy than the alkyl sp³ orbital, the $|\beta|$ value is reasonably considered to be smaller than the ($\epsilon_A - \epsilon_B$) value in the metal−alkyl bond. The electron-withdrawing substituent on the sp³ C atom stabilizes the alkyl sp³ orbital in energy, and therefore, the ($\epsilon_A - \epsilon_B$) term becomes larger, which increases the ΔE_{bond} value. Thus, eq 11 provides a clear explanation for the fact that the Pt−alkyl bond becomes strong by incorporating an electron-withdrawing substituent on the sp³ C atom. As shown in Table 5, the sp³ orbital energy of CH₃ is the most stable. If we adopted the above explanation, the Pt−CH₃ bond would be the strongest. This explanation is against our present computational results. In this case, therefore, we need to investigate various factors in detail. One plausible factor is the orbital overlap; the CH₃ sp³ orbital yields smaller overlap with Pt 5d$_\sigma$, 6s, and 6p$_\sigma$ orbitals than the sp³ orbital of SiH₃, GeH₃, and SnH₃, as shown in Table 6. As a result, the M−CH₃ bond energy is smaller than the M−SiH₃, M−GeH₃, and M−SnH₃ bond energies.

A comparison among M−SiH₃, M−GeH₃, and M−SnH₃ bonds is also interesting. Although the bond energy difference among them is not very large, both the first bond dissociation energy and the average bond energy of the M−XH₃ bond decrease in the order M−SiH₃ > M−GeH₃ > M−SnH₃. The sp³ orbital energy becomes lower in the order SnH₃ > GeH₃ > SiH₃, and the
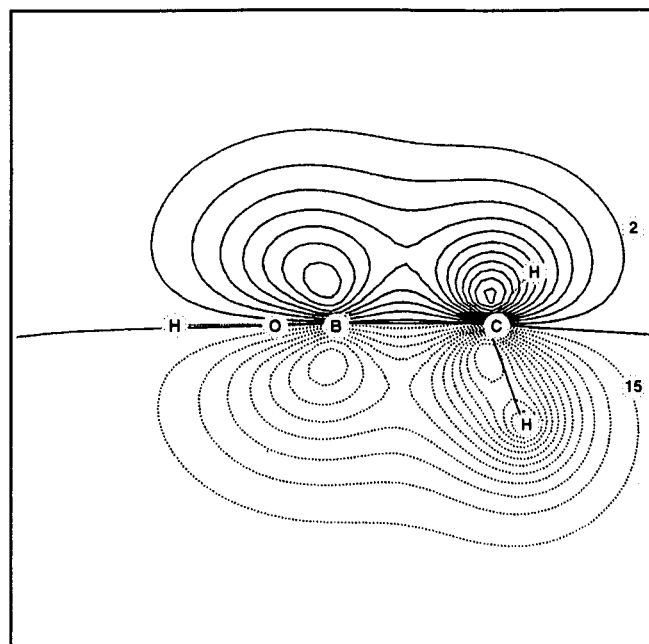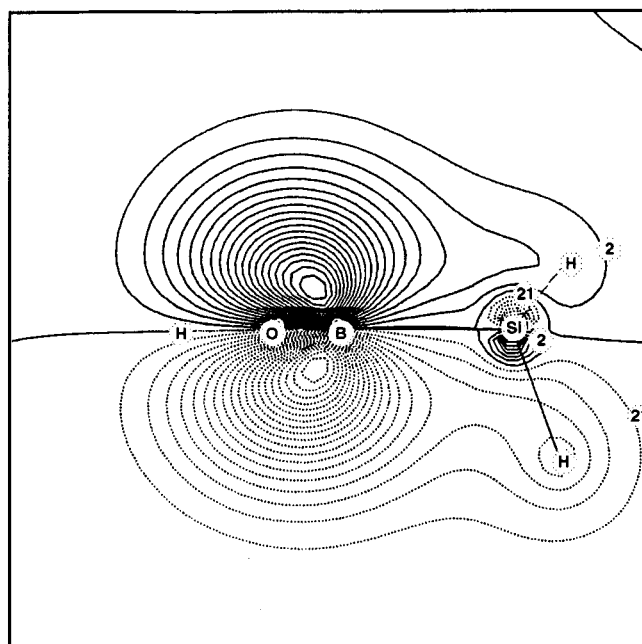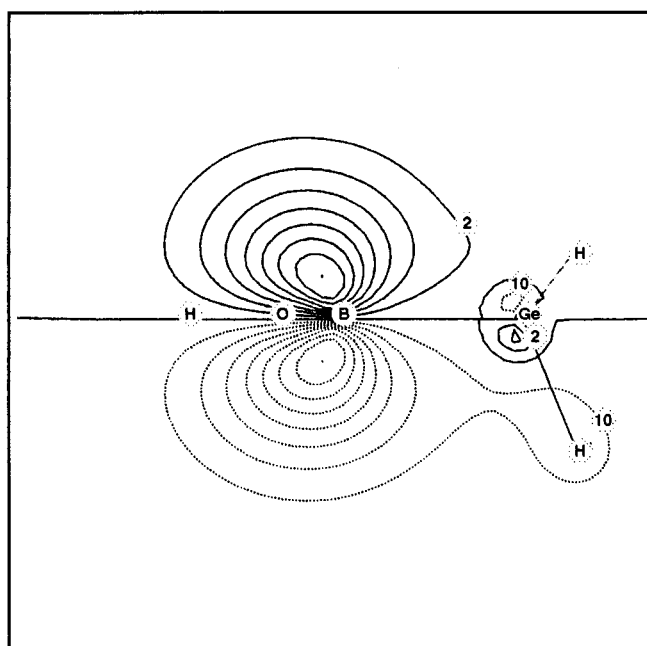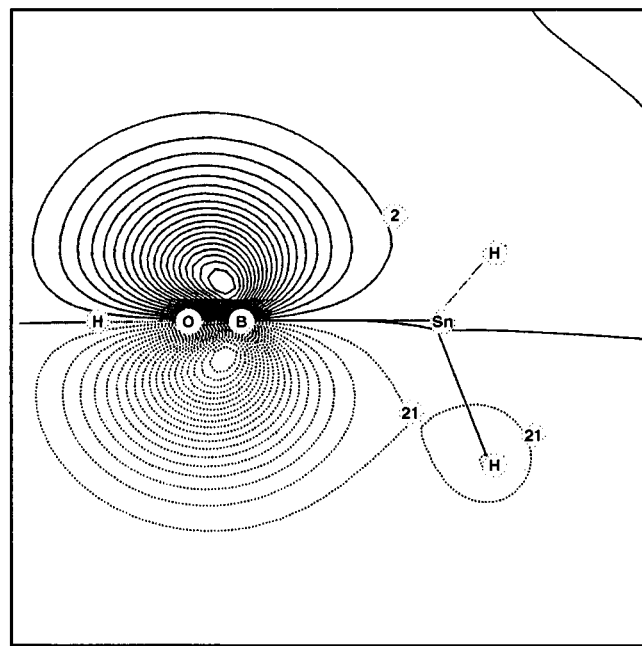
(A) (HO)₂B-CH₃

(B) (HO)₂B-SiH₃

(C) (HO)₂B-GeH₃

(D) (HO)₂B-SnH₃

Figure 6. Contour maps of the HOMO of $(HO)_2B-CH_3$, $(HO)_2B-SiH_3$, $(HO)_2B-GeH_3$, and $(HO)_2B-SnH_3$. (A) Contour values increase from 0.0125 by 0.0125 and decrease from -0.125 by 0.125. (B) Contour values increase from 0.005 by 0.005 and decrease from -0.005 by 0.005. (C) Contour values increase from 0.0125 by 0.0125 and decrease from -0.125 by 0.125. (D) Contour values increase from 0.005 by 0.005 and decrease from -0.005 by 0.005.

ionization potential increases in the same order. The orbital overlap between Pt d_{z^2} and XH_3 sp^3 orbitals decreases in the order $M-SiH_3 > M-GeH_3 > M-SnH_3$. All these factors lead to the decreasing order of the bond energy $M-SiH_3 > M-GeH_3 > M-SnH_3$.

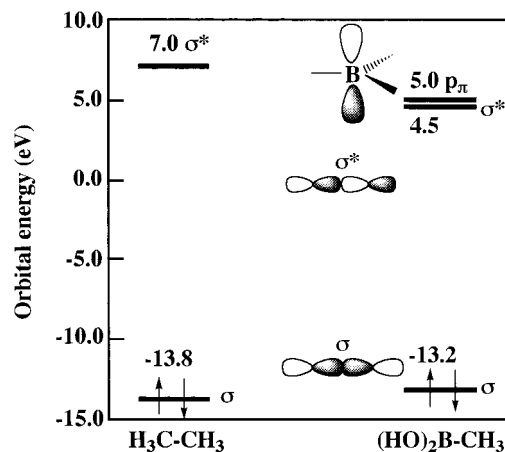**Interaction at the Transition State and Origin of the Activation Barrier.** In the transition states

TS1b, **TS2a**, and **TS2b** of oxidative additions of $(HO)_2B-SiH_3$ and $(HO)_2B-GeH_3$, Pt and Pd atomic populations considerably decrease and the $B(OH)_2$ population considerably increases, as shown in Figure 7. These population changes indicate that charge-transfer considerably occurs from Pt to the boryl group in the transition state. Usually, the charge transfer occurs from the metal
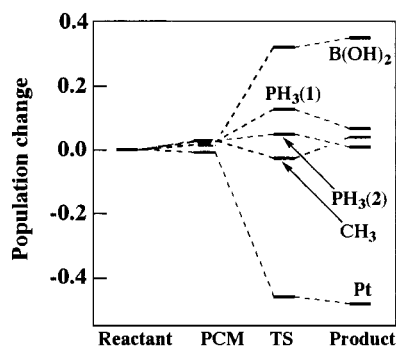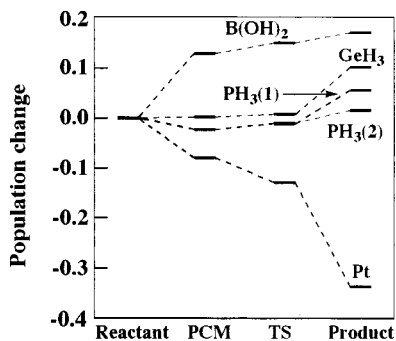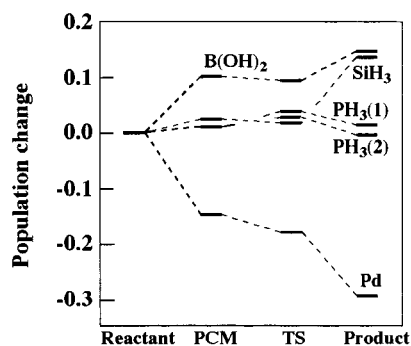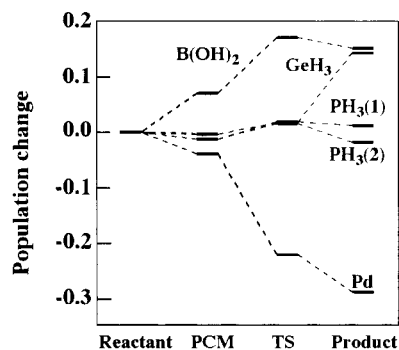
Figure 7. Population changes in the oxidative addition reactions of $(HO)_2B-CH_3$ and $(HO)_2B-GeH_3$ with $Pt(PH_3)_2$ and those of $(HO)_2B-SiH_3$ and $(HO)_2B-GeH_3$ with $Pd(PH_3)_2$.

Table 6. Overlap Integrals between M and XH_3 and between M and $B(OH)_2$[a]

	$\langle sp^3|5s\rangle$	$\langle sp^3|5p_z\rangle$	$\langle sp^3|d_{z^2}\rangle$
$Pd-B(OH)_2$	0.528	0.536	0.418
$Pd-CH_3$	0.339	0.329	0.323
$Pd-SiH_3$	0.501	0.516	0.349
$Pd-GeH_3$	0.508	0.530	0.336
$Pd-SnH_3$	0.478	0.479	0.297
$Pt-B(OH)_2$	0.543	0.538	0.485
$Pt-CH_3$	0.358	0.339	0.361
$Pt-SiH_3$	0.507	0.519	0.404
$Pt-GeH_3$	0.526	0.529	0.413
$Pt-SnH_3$	0.472	0.479	0.340

[a] These overlap integrals were calculated with minimal basis sets for Pd and Pt, using the Pt−X and Pd−X distances optimized for the products.

d orbital to the Y−Y σ^* orbital (Y = H, C, etc.) in the oxidative addition of the Y−Y σ-bond, as shown in Scheme 2A, which is necessary to break the Y−Y bond and to form the M−Y bond. However, the B−X bond breaking does not effectively occur in these transition states; for instance, the B−X bond lengthens only a little (Figures 1 and 4) and the eigenvector with imaginary frequency does not exhibit the B−X bond breaking (see above and Figure 5). Thus, the B−X σ^* orbital does not participate in the above-mentioned charge-transfer interaction. Besides B−X σ^* orbital, the boryl group has an empty p_π orbital at a slightly higher energy than the B−X σ^* orbital, as shown in Figure 8, and the p_π orbital expands perpendicularly to the molecular plane. This p_π orbital can form a strong charge-transfer interaction with the doubly occupied d orbital of M (M = Pd or Pt), as shown in Scheme 2C. This strong charge-transfer

Figure 8. Energy levels of the σ, σ^*, and p_π orbitals of CH_3-CH_3 and $(HO)_2B-CH_3$.

interaction results in the decrease of the M atomic population and the increase of the $B(OH)_2$ population described above and stabilizes the transition state.

The next issue to be investigated is the origin of activation barrier. Although B−X bond breaking does not occur effectively in these reactant-like transition states, $(HO)_2B-XH_3$ and $M(PH_3)_2$ moieties moderately distort, and their distortion gives rise to a destabilization energy, as shown in Table 7. Also, the approach of $(HO)_2B-XH_3$ causes energy destabilization due to the steric repulsion between $(HO)_2B-XH_3$ and $Pt(PH_3)_2$. Thus, the distortion energies of the $(HO)_2B-XH_3$ and $M(PH_3)_2$ moieties and the steric repulsion between $Pt-(PH_3)_2$ and $(HO)_2B-XH_3$ are responsible for the activa-
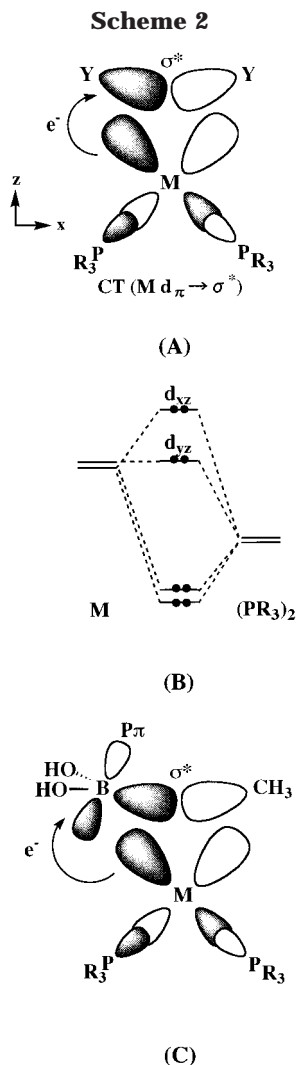
Scheme 2

CT (M $d_\pi \rightarrow \sigma^*$)

(A)

(B)

(C)

Table 7. Transition-State Character in the Oxidative Additions of CH_3-CH_3 and $(HO)_2B-XH_3$ Bonds to $Pt(PH_3)_2$ and $Pd(PH_3)_2$

	$Pt(PH_3)_2$			$Pd(PH_3)_2$	
	CH_3- CH_3	$(HO)_2B-$ CH_3	$(HO)_2B-$ GeH_3	$(HO)_2B-$ SiH_3	$(HO)_2B-$ GeH_3
$\Delta R(B-X/\text{Å})$	0.499	0.131	0.026	0.122	0.080
$\Delta E_{dist}(M)^a$	16.0	17.0	1.2	7.5	2.5
$\Delta E_{dist}(B-X)^a$	54.8	29.3	4.3	13.2	9.6
$\Delta q(B-X)^b$	0.163	0.290	0.152	0.201	0.189

^{a} kcal/mol (MP4SDQ). ^{b} Population change of $(HO)_2B-XH_3$ relative to the reactant. A positive value means an increase in the population.

tion energy. These destabilization energies are compensated with the charge-transfer interaction between $M(PH_3)_2$ and the boryl group, which leads to a small activation energy of the oxidative additions of $(HO)_2B-SiH_3$ and $(HO)_2B-GeH_3$ and no activation energy of the oxidative addition of $(HO)_2B-SnH_3$.

TS1a of the oxidative addition of $(HO)_2B-CH_3$ to $Pt(PH_3)_2$ is considerably different from the others, as follows: (1) in this transition state, the B−C bond substantially lengthens and the geometry is nearly planar, and (2) distortion energies of $(HO)_2B-CH_3$ and $Pt(PH_3)_2$ are significantly larger than the others. Consistent with these geometrical features, the eigenvector with imaginary frequency involves B−C bond breaking.

From these features, it is reasonably concluded that B−C bond breaking is mainly responsible for the activation barrier. This is because the B−C bond is much stronger than the B−Si, B−Ge, and B−Sn bonds (see Table 3).

A comparison between $(HO)_2B-CH_3$ and CH_3-CH_3 is of considerable interest, since the oxidative addition of $(HO)_2B-CH_3$ to $Pt(PH_3)_2$ occurs with a much smaller E_a value than that of CH_3-CH_3, despite the similar endothermicity of these reactions (Table 2). It should be noted in Table 7 that the distortion energy of CH_3-CH_3 is much larger than that of $(HO)_2B-CH_3$. This large distortion energy mainly arises from the significant C−C bond elongation (see ΔR in Table 7). The reason for the C−C bond elongation is easily interpreted in terms of the charge transfer to the C−C σ^* orbital from Pt, which necessarily occurs in the transition state, as shown in Scheme 2A; since the C−C σ^* orbital is at a much high energy (Figure 8), the C−C bond elongation must occur to lower the σ^* orbital in energy so as to form efficiently the charge-transfer interaction. On the other hand, the p_π orbital of $(HO)_2B-CH_3$ receives electrons from Pt to a greater extent than CH_3-CH_3 in the transition state despite the lesser extent of B−X bond elongation. The other important difference is that the stabilization energy (ΔE_{stab}) produced by the interaction between $Pt(PH_3)_2$ and $(HO)_2B-CH_3$ in the transition state is much larger than the ΔE_{stab} value by the interaction between $Pt(PH_3)_2$ and CH_3-CH_3: $\Delta E_{stab} = 14.5$ kcal/mol for CH_3-CH_3 and 29.1 kcal/mol for $(HO)_2B-CH_3$, where $\Delta E_{stab} = E_t(A_{dist}) + E_t(B_{dist}) - E_t(A-B)_{TS}$ and A_{dist} means the fragment A whose structure is distorted like that in the transition state. The above results clearly show that some bonding interaction stabilizes the transition state of the B−C oxidative addition. The boryl p_π orbital is responsible for all these features of the $(HO)_2B-CH_3$ oxidative addition such as the smaller distortion energy, the larger increase of the electron population of $(HO)_2B-CH_3$, and the larger ΔE_{stab} value, as follows: The empty p_π orbital of the boryl group forms a charge-transfer interaction with the doubly occupied d orbital of Pt (Scheme 2C), which stabilizes to a great extent the transition state and leads to the above-mentioned electron distribution. Because of the presence of the boryl p_π orbital, the B−C bond does not need to lengthen very much in the transition state so as to enhance the charge-transfer interaction with Pt, which does not give rise to a large distortion energy. Thus, it should be reasonably concluded that the empty p_π orbital of boryl plays a crucial role in performing the B−C oxidative addition with a lower E_a value than that of CH_3-CH_3. In other words, CH_3-CH_3 must distort very much to form effectively the charge-transfer interaction with Pt because it does not have such an empty p_π orbital. As a result, the E_{stab} value is small, the electron population of CH_3-CH_3 increases to a lesser extent, and the E_a value becomes very large.

The greater reactivity of $(HO)_2B-SiH_3$ than that of CH_3-SiH_3 (see above and Table 2) is similarly interpreted in terms of the boryl p_π orbital. CH_3-SiH_3 does not have an empty p_π orbital, and therefore, it needs to distort very much at the transition state, which leads to a large activation energy.

Scheme 3

Scheme 4

Planar   **Non-planar**
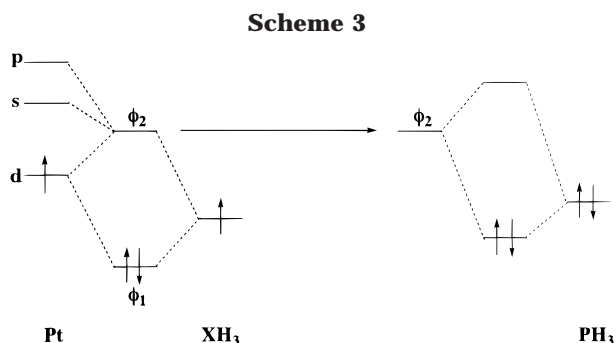
Strong Trans Influence of B(OH)₂. As discussed above, the trans influence of $B(OH)_2$ is much stronger than those of CH_3, SiH_3, GeH_3, and SnH_3. Considering that the trans influence of the silyl group is very strong,[32] it should be noted that the boryl group exhibits a surprisingly strong trans influence. The strong trans influence of the boryl group was experimentally reported, too; the NMR coupling constant $J_{Pt−P}$ in the Pt-(II) complex decreases with an increase of trans influence of the ligand that is at a position trans to phosphine, and this value decreases in the order Cl ≫ Ph > Bcat (cat = catechol), indicating that the trans influence of boryl is stronger than that of Ph.[10]

The strong trans influence of silyl group is easily interpreted in terms of orbital energy of SiH_3. As shown in Table 5, the sp³ orbital of SiH_3 lies at a much higher energy than that of CH_3. As a result, the SiH_3 sp³ orbital provides considerable bonding mixing with Pt d, s, and $p_σ$ orbitals and pushes up the $φ_2$ orbital in energy, as shown in Scheme 3, where $φ_2$ is an antibonding orbital which consists of Pt d, s, and $p_σ$ and SiH_3 sp³ orbitals. Since PH₃ donates its lone pair electrons to this $φ_2$ orbital to form the M−PH₃ coordinate bond, the electron donation of PH₃ is more suppressed and the bonding interaction between the PH₃ lone pair and $φ_2$ orbitals becomes weaker in the silyl complex than in the methyl complex.

A similar discussion might be applied to the explanation of the strong trans influence of the boryl group. Since we had better consider the orbital relaxation in discussing the bond formation, the ionization potential (I_p) is a better measure of energy level than the orbital energy. Although the $B(OH)_2$ sp² orbital is at a slightly lower energy than the SiH_3 sp³ orbital, the I_p value of $B(OH)_2$ is smaller than that of SiH_3 (Table 5). Thus, the $B(OH)_2$ sp² orbital is considered to be at a higher energy than the SiH_3 sp³ orbital. Also, the $B(OH)_2$ sp² orbital overlaps well with the Pt s and $p_σ$ orbitals to a greater extent than the SiH_3 sp³ orbital (Table 6), probably because the Pt−B distance is short due to the π-back-donation between the Pt $d_π$ and boryl $p_π$ orbitals. Thus, the $B(OH)_2$ sp² orbital forms a stronger covalent bond with the Pt d, s, and $p_σ$ orbitals than does the SiH_3 sp³ orbital from the two points of view of orbital energy difference and orbital overlap. As a result, $B(OH)_2$ pushes up the $φ_2$ orbital in energy to a greater extent than SiH_3, and the trans influence of $B(OH)_2$ is stronger than that of SiH_3.[33]

Geometry of the Transition State of CH₃−B-(OH)₂ Oxidative Addition to Pt(PH₃)₂. Only the
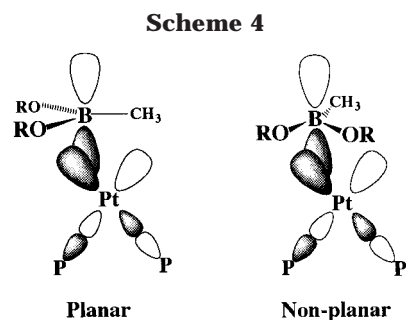
transition state of the oxidative addition of $(HO)_2B−CH_3$ to $Pt(PH_3)_2$ is nearly planar, as shown in Figure 1, while the other transition states optimized here are completely nonplanar. In our previous theoretical study of the Si−C oxidative addition to $Pt(PH_3)_2$,[25] we reported that the nonplanar transition state is favorable from the point of view of a steric factor, but the planar structure is favorable from the point of view of an electronic factor. Also, the intrinsic reaction coordinate (IRC) calculation clearly showed that the geometry of $Pt(PH_3)_2(CH_3−SiH_3)$ becomes planar in the late stage of the reaction.[25] Thus, the planar structure of **TS1a** is consistent with the fact that **TS1a** is product-like (vide supra). Since **TS1a** is product-like, Pt−B and Pt−C bond formation and B−C bond breaking occur to a considerable extent in the transition state. To form the Pt−B and Pt−C bonds and to break the B−C bond, charge transfer from the Pt $d_π$ to the B−C σ* orbital must occur. The planar transition state is favorable for the charge-transfer interaction because the planar transition state provides overlap between the B−C σ* orbital and the Pt $d_π$ orbital, which is at a higher energy than the other $d_π$ orbital, as shown in Scheme 2A and 2B. Thus, **TS1a** is nearly planar.

In the oxidative addition reactions of the other substrates such as $(HO)_2B−SiH_3$ and $(HO)_2B−GeH_3$, the B−Si and B−Ge bonds only slightly lengthen at the transition state. This means that the B−X σ* orbital does not contribute to the charge transfer from the doubly occupied d orbital of M. Besides the charge transfer to the σ* orbital, the charge transfer from M to the $B(OH)_2$ $p_π$ orbital is important to stabilize the transition state, and this charge transfer efficiently occurs even in the nonplanar transition state because the boryl $p_π$ orbital can overlap with one lobe of the d orbital even in the nonplanar transition state, as shown in Scheme 4. As a result, the transition state becomes nonplanar.

Now, we examine the effects of steric repulsion of phosphine in the transition state of the $(HO)_2B−CH_3$ oxidative addition. Even when we substitute PH₂Me for PH₃, the transition state is still nearly planar, as shown in Figure 9, where the Me group is placed at the nearest position to $(HO)_2B−CH_3$. In this transition state, the B−C bond lengthens the least. This is probably because

---

(32) Chatt, J.; Shaw, B. L. *J. Chem. Soc.* **1959**, 4020.

(33) In this discussion, we do not need to consider the possibility that the empty $p_π$ orbital of boryl directly weakens the coordinate bond of PH₃. If a ligand at a position trans to boryl forms a π-back-donating interaction with the central metal, the π-back-donating interaction the boryl group directly weakens the coordinate bond of the trans ligand. However, the π-back-donation does not participate in the coordination of PH₃, since PH₃ does not have a π-acceptor orbital. Thus, the Pt−PH₃ bond is not directly weakened by the back-donation of the boryl group.

Figure 9. Geometry changes in the oxidative addition of $(HO)_2B-CH_3$ to $Pt(PH_2Me)_2$ and $Pt(PH_2Et)_2$. Bond distances in angstroms and bond angles in degrees. We could not optimize the precursor complex when phosphine was PH_2Et.

Table 8. Activation Energy (E_a) and Reaction Energy (ΔE) of Oxidative Addition of $(HO)_2B-CH_3$ to $Pt(PH_2R)$

	H	Me	Et
$E_a{}^a$	21.5	22.8	30.8
ΔE^a	3.0	3.5	14.2

^{a} kcal/mol. MP4SDQ calculation.

the B–C bond does not need to lengthen very much due to the stronger donating ability of PH_2Me than that of PH_3; in other words, because of the stronger donating ability of PH_2Me, $Pt(PH_2Me)_2$ is able to form effectively the charge-transfer interaction between Pt d and $(HO)_2B-CH_3$ even if the B–C bond does not lengthen very much.

When we substitute PH_2Et for PH_3, the transition state completely changes to a nonplanar structure; the dihedral angle between the B–C bond and the PtP_2 plane is 64°, as shown in Figure 9, where the Et group is placed at the nearest position to $(HO)_2B-CH_3$. This is because PH_2Et causes steric repulsion with $(HO)_2B-CH_3$. In this TS, the B–C bond lengthens the most. This is interpreted in terms of the charge-transfer interaction between the Pt d_π and B–C σ^* orbitals, as follows: Since the Pt d_π orbital, which is at a higher energy than the others, cannot overlap with the B–C σ^* orbital in the nonplanar geometry, the nonplanar transition state is not favorable for the charge-transfer interaction, and therefore, the B–C bond of $(HO)_2B-CH_3$ must lengthen to recover the charge-transfer interaction. These results suggest that the transition-state structure is flexible and sensitive to the electronic and steric factors.

The E_a and ΔE values are summarized in Table 8. Apparently, E_a and ΔE change little upon going from PH_3 to PH_2Me. However, E_a and ΔE increase greatly upon going from PH_2Me to PH_2Et. From these results one might predict that the small phosphine is favorable

for the oxidative addition. Actually, $P(OCH_2CH_2)_3CH$, which is considered less bulky, was successfully used for several catalytic reactions that involve the oxidative addition reactions.[34]

Conclusions

Oxidative addition of $(HO)_2B-XH_3$ to $Pt(PH_3)_2$ occurs with a moderate activation energy for X = C, and either a very small barrier or no barrier for X = Ge, Si, and Sn. Also, oxidative addition of $(HO)_2B-XH_3$ to $Pd(PH_3)_2$ occurs with either a very small barrier or no barrier for X = Si, Ge, and Sn, whereas only the oxidative addition of $(HO)_2B-CH_3$ to $Pd(PH_3)_2$ cannot take place, but the reductive elimination of $(HO)_2B-CH_3$ from the Pd(II) complex occurs with no barrier.

The bond energy decreases in the order B–C > B–Si > B–Ge > B–Sn, M–B(OH)$_2$ > M–SiH$_3$ > M–GeH$_3$ > M–SnH$_3$ > M–CH$_3$, Pt–B(OH)$_2$ > Pd–B(OH)$_2$, and Pt–XH$_3$ > Pd–XH$_3$. The fact that the M–B(OH)$_2$ bond is stronger than the M–SiH$_3$, M–GeH$_3$, and M–SnH$_3$ bonds is interpreted in terms of the π-back-donating interaction between the M d_π and B(OH)$_2$ p_π orbitals.

Since the B–C bond is the strongest in all the B–X bonds and the Pt–CH$_3$ bond is the weakest in all the Pt–XH$_3$ bonds, the oxidative addition of $(HO)_2B-CH_3$ to $Pt(PH_3)_2$ requires a moderate activation energy and is slightly endothermic. The oxidative addition of $(HO)_2B-CH_3$ to $Pd(PH_3)_2$ is difficult, because the Pd–CH$_3$ and Pd–B(OH)$_2$ bonds are much weaker than the Pt–B(OH)$_2$ and Pt–CH$_3$ bonds, respectively. On the other hand, $(HO)_2B-SiH_3$, $(HO)_2B-GeH_3$, and $(HO)_2B-$

(34) Yamashita, H.; Catellani, M.; Tanaka, M. *Chem. Lett.* **1991**, 241. Yamashita, H.; Reddy, N. P.; Tanaka, M. *Chem. Lett.* **1993**, 315. Yamashita, H.; Tanaka, M. *Bull. Chem. Soc. Jpn.* **1995**, *68*, 403.

SnH$_3$ undergo oxidative addition to Pt(PH$_3$)$_2$ with significant exothermicity and either a very small barrier or no barrier, because the B−Si, B−Ge, and B−Sn bonds are much weaker than the B−C bond and the Pt−SiH$_3$, Pt−GeH$_3$, and Pt−SnH$_3$ bonds are stronger than the Pt−CH$_3$ bond. These substrates also undergo oxidative addition to Pd(PH$_3$)$_2$ with either a very small barrier or no barrier, while they are much less exothermic than those to Pt(PH$_3$)$_2$, because Pd−B(OH)$_2$ and Pd−XH$_3$ bonds are much weaker than Pt−B(OH)$_2$ and Pt−XH$_3$ bonds, respectively.

The B−C bond is stronger than the C−C bond, because the hyperconjugation between the C−H σ orbital of CH$_3$ and the p$_\pi$ orbital of B(OH)$_2$ participates in the B−C bond. Despite the strong B−C bond, (HO)$_2$B−CH$_3$ undergoes oxidative addition to Pt(PH$_3$)$_2$ with a much smaller activation energy than does CH$_3$−CH$_3$. Since the endothermicity is similar in these two oxidative addition reactions, the product stability is not responsible for the smaller activation energy of the (HO)$_2$B−CH$_3$ oxidative addition. B(OH)$_2$ has an empty p$_\pi$ orbital, which participates in a charge-transfer interaction with the Pt d orbital at the transition state. This charge-transfer interaction stabilizes the transition state of the (HO)$_2$B−CH$_3$ oxidative addition, while the transition state of the CH$_3$−CH$_3$ oxidative addition cannot be stabilized at all by this charge-transfer interaction because of the absence of the empty p$_\pi$ orbital in CH$_3$−CH$_3$. In all the oxidative additions of (HO)$_2$B−XH$_3$, the electron distribution clearly shows the participation of this charge-transfer interaction in the transition state. In other words, the boryl p$_\pi$ orbital is responsible for the high reactivity of (HO)$_2$B−XH$_3$ in the oxidative addition reaction.

The transition states of these oxidative additions are nonplanar except for the nearly planar TS of the oxidative addition of (HO)$_2$B−CH$_3$ to Pt(PH$_3$)$_2$. This nearly planar TS structure is sensitive to electronic and steric factors; for instance, when PH$_3$ is replaced by PH$_2$-Et, the TS becomes nonplanar to decrease the steric repulsion between (HO)$_2$B−CH$_3$ and PH$_2$Et.

Also, it should be noted that the trans influence of the boryl group is very strong; it is stronger than the strong trans influence of silyl group. This is because the B(OH)$_2$ sp^2 orbital is at a higher energy and provides larger overlap with Pt s and p orbitals than does the SiH$_3$ sp^3 orbital. The good overlap between B(OH)$_2$ sp^2 and Pt d, s, and p orbitals would arise from the rather short M−B distance for which the π-back-donating interaction between M and B(OH)$_2$ is responsible.

In conclusion, it is clearly shown here that the boryl p$_\pi$ orbital plays a crucial role in the M−boryl bonding and oxidative addition to transition metal complexes.